Analysis of Hurricanes Using Long-Range Lightning Detection Networks

BENJAMIN TRABING

University of Oklahoma/NSSL, Norman, OK

JOHN A. KNAFF

NOAA Center for Satellite Applications and Research, Fort Collins, CO

ANDREA SCHUMACHER AND KATE MUSGRAVE

CIRA/ Colorado State University, Fort Collins, CO

MARK DEMARIA

NWS/National Hurricane Center, Miami, FL

* *Corresponding Author*:
Benjamin Trabing, University of Oklahoma/NSSL, 120 David L. Boren Blvd., Suite 5900, Norman, OK 73072, benjamin.trabing@noaa.gov

Abstract

The new GOES-R satellite will be equipped with the Geostationary Lightning Mapper (GLM) that will provide unprecedented total lightning data with the potential to improve hurricane intensity forecasts. Past studies have provided conflicting interpretations of the role that lightning plays in forecasting tropical cyclone (TC) intensity changes. With the goal of improving the usefulness of total lightning, detailed case studies were conducted of five TCs that underwent rapid intensification (RI) within the domains of two unique ground-based long-range lightning detection networks, the World Wide Lightning Location Network (WWLLN) and Earth Networks Total Lightning Network (ENTLN). This analysis will provide greater details of the distribution of lightning within predefined storm features to highlight specific phenomena that large statistical studies cannot resolve.

Both WWLLN and ENTLN datasets showed similar spatial and temporal patterns in lightning that validates the independent use of either network for analysis. For the cases examined, a maxima in eyewall lightning was located downshear and in the front-right quadrants relative to storm motion. Results show that RI follows a burst of lightning in the eyewall when coinciding with a period of little environmental vertical shear. Eyewall lightning would cycle with greater frequency during intensification compared to weakening. Bursts of lightning were observed in the eyewall just prior to eye formation in both the infrared and microwave imagery. Eyewall lightning bursts in low shear environments could be used to indicate intensification and improve forecasts.

1. **Introduction**

Tropical cyclones have the capacity to devastate coastal communities not only in the tropics but in the mid latitudes as well. It is important to keep increasing the accuracy and precision of forecasts to ensure that the proper decisions are made by emergency management teams located in the storms' path. Increasing the accuracy of forecast models is an important part of this process, especially the short-term intensity forecasts. Short-term intensity forecasts, those within the next 24 hours, are the most critical in determining the risks associated with an approaching TC. Official intensity forecast errors for 24-h forecasts have shown only slight improvements in skill in the last decade (Cangialosi and Franklin, 2014) and in response, modest improvements in intensity guidance (DeMaria et al. 2014). Since TCs are not easily accessible to make in situ measurements, lightning, which is fundamentally related to moist convection and can be detected remotely, could be a valuable tool in decreasing this forecast error in the future.

Many studies have shown that lightning can give important information into the convective structure of TCs. Black and Hallet (1999) showed that there is a distinction between electrically weak and active hurricanes relating to the presence of weak and strong updrafts. Previous studies have produced conflicting results on the role that total lightning plays as a signal for tropical cyclone intensity change. Molinari et al. (1994) found that in Hurricane Andrew there was an outbreak of lightning in the eyewall prior to each and every intensification period. An analysis of Hurricanes Katrina and Rita by both Solorzano et al. (2008) using the World Wide Lightning Location Network (WWLLN; Rodger et al. 2006) and Squires and Businger (2008) using the National Lightning Detection Network (NLDN), showed eyewall lightning outbreaks during the periods of rapid intensification (RI). Abarca et al. (2011) found in 24 Atlantic TCs that lightning in the inner core has the potential to distinguish intensifying versus non-intensifying storms. DeMaria et al. (2012) found contradictory results using six-hourly WWLLN-based lightning density to analyze rapid intensity changes in TCs from 2005 to 2010 in both the Atlantic and East Pacific basins. The study found that storms with eyewall lightning tended to decrease in intensity during the following 24 hours while those same TCs with rainband lightning tended to increase in intensity during the following 24 hours. This study also found that strong vertical wind shear is related to the greatest lightning activity in the eyewall region and that those cases often subsequently weakened.

In 2016, the next generation (i.e., R-series) Geostationary Orbiting Environmental Satellite (GOES-R; http://www.goes-r.gov/spacesegment/instruments.html) will be launched. This satellite will be equipped with the Geostationary Lightning Mapper (GLM; Goodman et al. 2013) that will provide continuous total lightning density measurements with nearly uniform spatial resolution. The GLM will provide an unprecedented look at lightning within TCs in either the GOES-East of GOES-West domain. In preparation for this new forecasting and research tool, this study analyzes hourly total lightning activity of several TC cases, exploring the use of this new data for TC intensity change forecasts by using ground-based long-range lightning detection networks as a proxy.

2. **Data and Methodology**

In this study, the WWLLN and Earth Networks Total Lightning Network (ENTLN; http://www.earthnetworks.com/Products/TotalLightningNetwork.aspx) were used to analyze five tropical cyclones that traversed both long-range lightning network's domains. The storms were selected for this study based on the conditions that rapid intensification (RI) occurred while in range of both networks. Figure 1 shows the tracks of the analyzed storms and their proximity to land. Similar to Kaplan et al. (2010), RI is defined as an increase of 25 kts in 24 hours. These storms were then analyzed in conjuncture with infrared (IR) and microwave (MI) satellite imagery, and deep layer (850 hPa to 200 hPa within a radius of 500 km) vertical wind shear magnitude and direction from the Statistical Hurricane Intensity Prediction Scheme (SHIPS; DeMaria et al. 2005) diagnostic files (SHIPS, cited 2015). Storm center location and intensity was taken from the National Hurricane Center (NHC) Best Track dataset when available. For the most recent storms, preliminary center and intensity measurements from the NHC were used. The storm track, intensity, and shear was linearly interpolated hourly to better co-locate storm center and the lightning data.

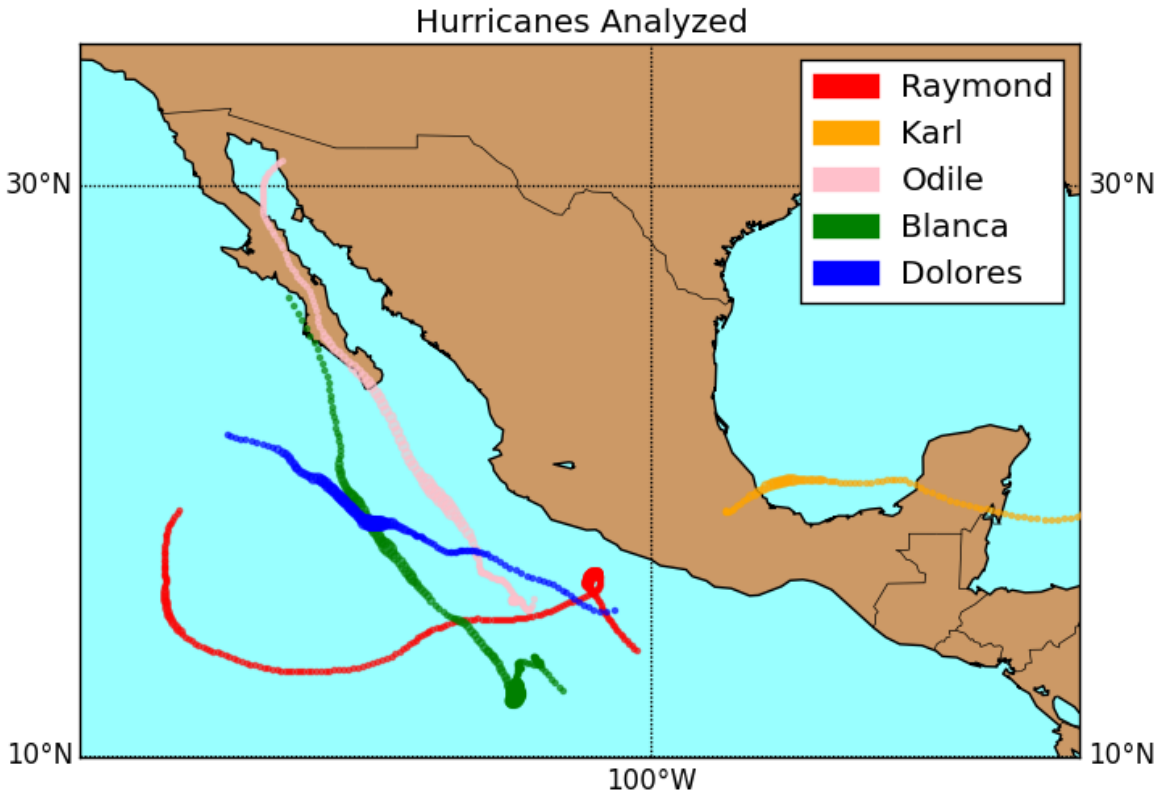

Figure 1: Tracks of the five major hurricanes examined in this study. The thickness of the points indicates strength of the storm and the closeness of points is proportional to its speed.

The WWLLN has a broad domain with relatively few sensors that encompass the globe. WWLLN detects very low frequency (VLF) radio waves between 3-30 kHz which detects mostly cloud-to-ground (CGs) discharges that radiate strongest in this range (Dowden 2002). Intra-cloud (IC) flashes have a weaker peak current and so are not often detected by the network. WWLLN allows for consistent analysis of tropical cyclones in any basin; because of the spatial distribution of the sensors. In a comparison with the Lightning Imaging Sensor (LIS) on the Tropical Rainfall Measuring Mission (TRMM) satellite, Rudlosky (2014) found that WWLLN had a detection efficiency (DE) of 17.3% over the ocean and 10.7% over North America. The network does not have the same consistency over landmasses, which results in inconsistencies when TCs interact with land. Because the network does not identify differences in flash type, most of its detected flashes are assumed to be CGs with few strong IC flashes mixed in.

Similar to WWLLN, ENTLN features global coverage with a high density of stations located in CONUS, Alaska, Hawaii, the Caribbean basin, Australia, and Brazil. ENTLN detects

total lightning activity using wideband sensors with a detection frequency ranging from 1 Hz to 12MHz (Rudlosky 2014). Because of the frequency range, both CGs and ICs can be detected, but a dense network of sensors is needed. ENTLN has a high DE over land masses including North America, but the DE drops off drastically at locations further off the coast away from sensors. Rudlosky (2014) found that ENTLN has a DE of 60.1% over North America which drops to 35.6% across the oceans. Because ENTLN has a higher DE closer to land, the TCs chosen for this study required paths close to the coast in areas of >50% DE. ENTLN is unique in its classification of flashes as IC or CG, however the accuracy of this classification over the ocean away from high density networks is questionable (e.g., Mallick et al. 2014). After analyzing the radial distribution of flash types in Figure 2, a high ratio of CG to IC flashes were found hundreds of kilometers of the coast of Mexico near Odile's center which reduced our confidence that ENLTN is providing total lightning.

An examination of the two networks reveals that both ENTLN and WWLLN were in agreement and provided the same results in this study. ENTLN detected more flashes than WWLLN because it was detecting total lightning in some areas, and both networks produced collocated flashes. A spatial analysis of the networks overlaid on satellite imagery showed the

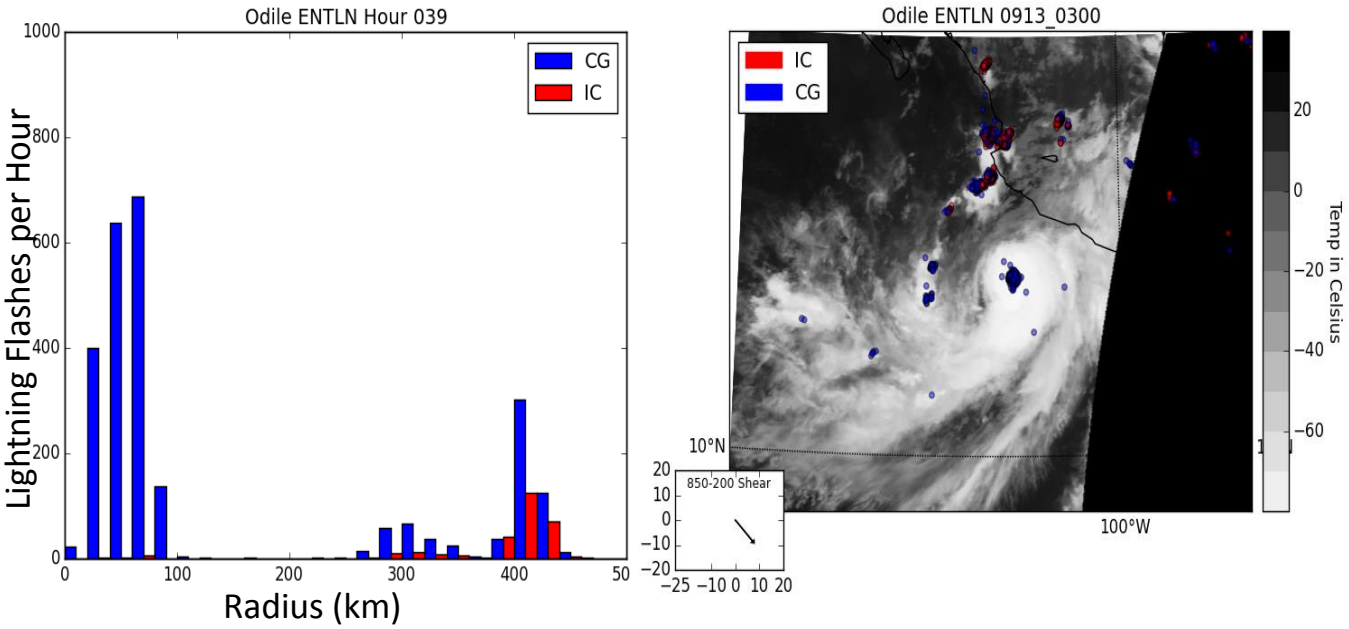

Figure 2: Right is a spatial analysis of the flash classification used by ENTLN for an hour time period in Hurricane Odile. Left shows the flashes binned at 20km intervals away from the storm center. Few IC flashes were detected within 280 km of the storm center corresponding to an area >200km away from the coast of Mexico.

consistency of the two networks and can be seen in Figure 3. From the analyzed satellite imagery, flashes were almost always associated with convective features. Both WWLLN and ENTLN datasets showed similar patterns in lightning that validates the independent use of either network for analysis. The ENTLN and WWLLN are well correlated in time and space, but the WWLLN detection efficiency is more spatially uniform over the open ocean. Since the WWLLN is providing essentially the same information without the variable DE, ENTLN data was not further used in our analyses.

For the five storms that were analyzed, the size of the eyewall, inner core, and rainbands were estimated. The eyewall and inner core were categorized as the region from 0 to50 km and 0 to 100 km extending radially from the storm center, respectively, following DeMaria et al. (2012). These storm features are consistent with past studies and applicable to all storms analyzed. The rainband region ranges from 150 to 450 km to accommodate the sized of the storms studied. This rainband region is used to resolve all the flashes that occur in the inner and outer rainband region of each storm while allowing for changes in storm size. A static parameterization of storm features was used to streamline results towards potential operational use. The storms analyzed in this study all occur within the past five years when the WLLNN had the most stations and highest DE (Rudlosky and Shea 2013; Rodger et al. 2014).

This study will examine the location of lightning as reported by WWLLN relative to storm motion and shear. A spatial analysis of lightning within each TC will be conducted by overlaying the lightning with enhanced (grayscale) digital IR. Azimuthal averages of lightning

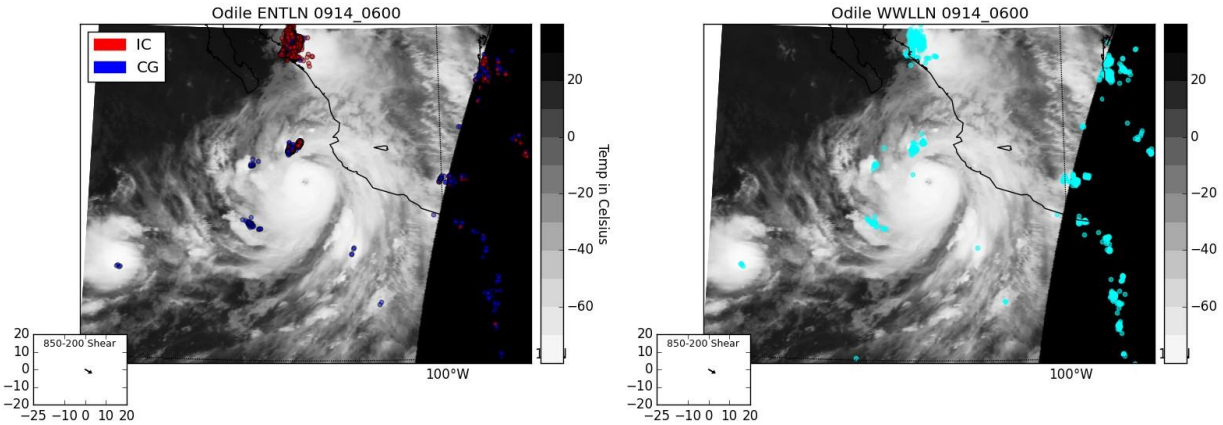

Figure 3: The similar spatial distribution of lightning during Hurricane Odile using ENTLN (left) and WWLLN (right).

within the predefined storm regions will give a better understanding of the changing lightning patterns over the desired time periods shown in Table 1. We will also take a closer look at the positioning of lightning within the eyewall and its relation to shear and storm motion vectors during major structural changes of each storm. The eyewall was examined in more depth because it is the typical location of the strongest updrafts within the storm (e.g. Rogers et al. 2012) and its dynamical importance to intensification processes (Rogers et al. 2013).

Table 1: The examined storms in this study are from the last 5 years. The start and end time is the time period that was examined in this study. The periods of rapid intensification are 25 kts in 24 hours. The eye formation times in the MI and IR columns are at the earliest times found.

						Period of RI		Eye Formation Time	
Year	Basin	Storm	Start (UTC)	End (UTC)	Vmax (kts)	Start (UTC)	End (UTC)	IR (UTC)	MI (UTC)
2010	Atlantic	Karl	15 SEP 0000	18 SEP 0600	105	16 SEP 0000	17 SEP 1200	17 SEP 0145	16 SEP 0600
2013	East Pacific	Raymond	20 OCT 0000	30 OCT 0000	110	20 OCT 0000	22 OCT 0000	21 OCT 0115	20 OCT 2215
					90	26 OCT 1800	28 OCT 0600	27 OCT 1830	27 OCT 1545
2014	East Pacific	Odile	11 SEP 1200	16 SEP 1200	115	13 SEP 0000	14 SEP 1200	13 SEP 2200	13 SEP 1215
2015	East Pacific	Blanca	01 JUN 0000	08 JUN 0000	120	01 JUN 1800	04 JUN 0000	03 JUN 1000	02 JUN 0830
					115	05 JUN 1200	06 JUN 1200		
2015	East Pacific	Dolores	12 JUL 1200	17 JUL 1200	120	14 JUL 0000	15 JUL 1200	15 JUL 0030	14 JUL 0930

3. **Results**

Each TC in this study was examined individually in order to take into consideration the ocean-atmosphere interactions and environmental factors. A look into each storm separately allows for a closer look at the lightning emanating from convective features in a small area and time. The detailed case studies presented here are important for reconciling the results of large statistical studies (e.g., DeMaria et al. 2012) and single case studies (i.e., Molinari et al. 2014) and providing incite as to how lightning information can be better utilized to improve intensity forecasts. This study is unique in its use of multiple strong, but not extraordinarily strong TCs, compared to case studies of category five storms like Andrew, Rita, and Katrina (i.e., Molinari et al. 1994 and Squires and Businger 2008).

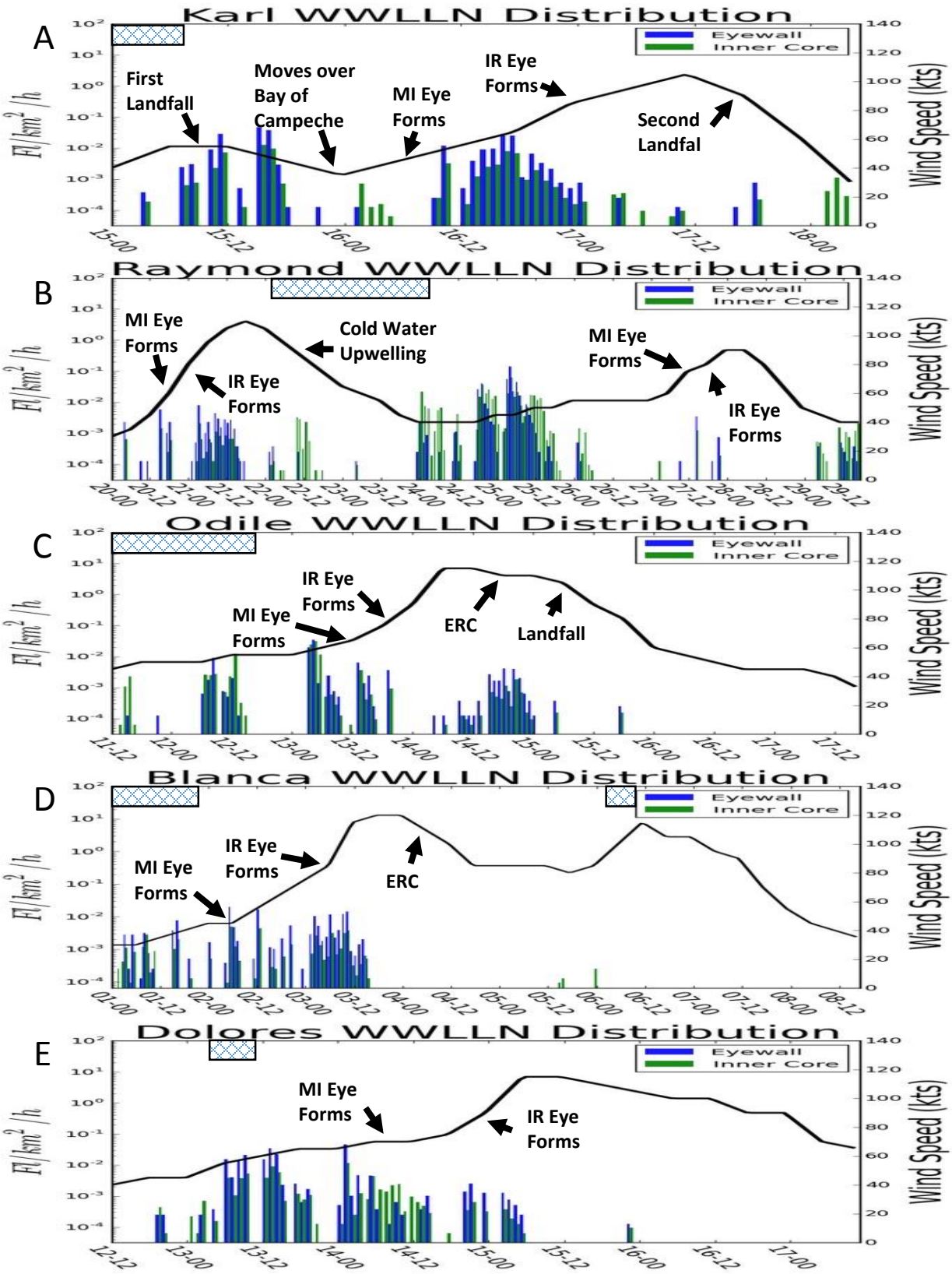

Figure 4: Temporal lightning distribution showing eyewall (blue) and inner core (green) lightning in Hurricanes Karl (A), Raymond (B), Odile (C), Blanca (D), and Dolores (E) in relation to wind speed. The blue hatched area at the top of each graph shows the time period where shear is >15 kts.

a. *Eyewall and Inner Core Lightning*

The temporal evolution in hourly intervals of our five cases can be seen in the entirety of Figure 4. Eyewall lightning was indicative of intense convection in each of the TCs. During the examined time periods of each of the five storms, lightning in the eyewall was found just prior to, during, and at the conclusion of RI in each and every TC. In the storms that underwent a second RI, Raymond and Blanca, lightning was again recorded in the eyewall during the second RI but in comparatively shorter bursts. Figure 4D shows that during the second RI period in Hurricane Blanca (05 Jun 1200 UTC to 06 Jun 1200 UTC), no eyewall lightning was recorded; however, Blanca had a much larger eye (64 km in the best track and 57 km RMW in the vortex message at 1813 UTC) and ragged looking IR eye during this time and so the burst of 'inner-core' lightning better represents the eyewall region during this period. The eyewall lightning in the second RI periods confirm that eyewall lightning is associated with intensification. Hurricane

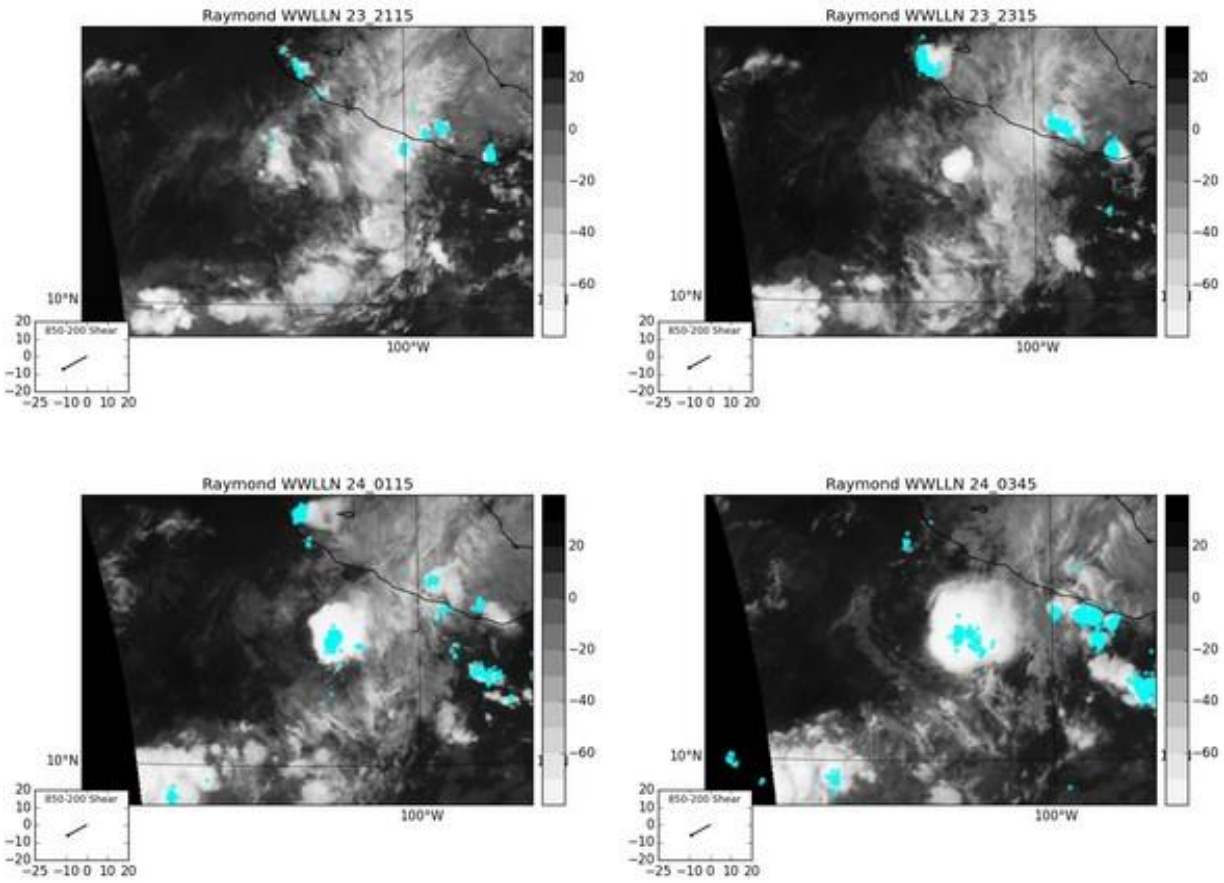

Figure 5: Hourly lightning progression of Hurricane Raymond following its downgrade to a tropical storm. Lightning near the center of circulation was evident of a rebirth of the system's convection. The vector in the lower left of each plot is the deep layer shear vector at that time.

Raymond also had a pronounced peak in lightning activity while it was a weak tropical storm from 24 Oct 0000 UTC through 26 Oct 1200 UTC (Figure 4B) which does not appear to occur during intensification. This lightning activity began after Raymond had lost all convection and was key to the reorganization of the TC as seen in the satellite imagery in Figure 5.

Bursts of lightning in the eyewall tended to pulse, so there are often breaks in lightning followed by a subsequent burst. During RI, eyewall lightning pulsated frequently with only 1-2 hour breaks in between, compared to an average between 6-8 hour breaks between pulses after RI had concluded. There was also a noticeable decline of eyewall lightning during the period of weakening in each TC. Albeit in the weakening of landfalling Hurricanes Karl and Odile, both storms had a single hour interval just after landfall in which eyewall lightning was recorded. A larger number of storms will need to be analyzed to determine if this 'final burst' is representative of the thermodynamic changes of TCs associated with landfall or just an anomaly.

In an analysis of eyewall lightning in relation to eye development, it was found that eyewall bursts occurred prior to the development of the eye in both the MI and IR satellite imagery. In Figure 6, the IR progresses in hourly intervals beginning at 13 Sep 1930 UTC with eyewall lightning evident. Following an hour with no observed lightning by either WWLLN or ENTLN in the eyewall, the eye starts to become visible at 13 Sep 2130 UTC. A pinhole eye can be definitively seen at 13 Sep 2230 UTC. The eye formation in the MI satellite imagery was estimated due to it being limited to near complete overpasses; however, the times listed in Table 1 and plotted in Figure 4 should provide viable estimations. Hurricane Karl was the only storm that did not exhibit eyewall lightning prior to the formation of its eye in the MI imagery, which could be caused by the proximity of the storm to land. In a further examination of Karl, an eye in the MI is present as the storm center moves off the Yucatán Peninsula and over the Bay of Campeche. Because of a lack of MI data during Karl's time over the Yucatán Peninsula, it's possible that the eye had formed several hours earlier. During each TC, eyewall lightning was present in a range of intervals leading up to eye formation in the IR. Each burst during the time

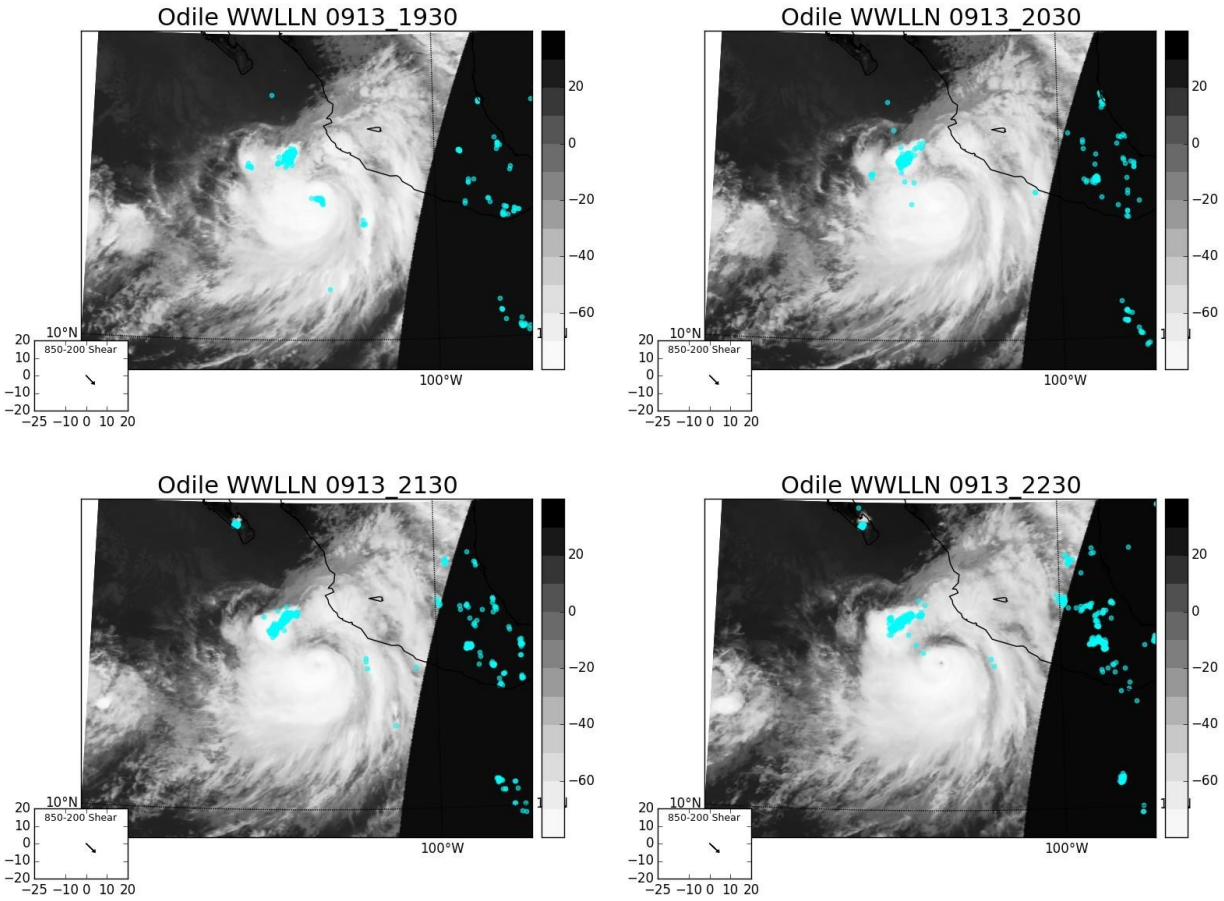

Figure 6: Hourly lightning progression of Hurricane Odile showing a burst of eyewall lightning prior to eye formation in IR imagery.

of eye formation in the IR was different. Hurricanes Odile and Delores had brief, one hour bursts just prior to IR eye formation, while Blanca and Raymond had eyewall lightning continue for several hours afterwards. Karl again was the exception as lightning in the eyewall concluded with the eye formation in the IR. Given the previous discussion, burst of eyewall and inner-core lightning also appear to be related to rapid changes in eyewall structure.

Next we analyzed the location of bursts of lightning within the eyewall of each storm. The lightning in each storm tended to be in the front-right quadrant relative to storm motion in the area of expected maximum wind speeds (Uhlhorn et al. 2014). These bursts seemed to occur only in azimuthal wavenumber one with lightning bursts occurring in only one quadrant at a given time. Some bursts would then begin to curve cyclonically, but would never make it completely around the storm as seen in Figure 8. This suggests that rotating organized updrafts

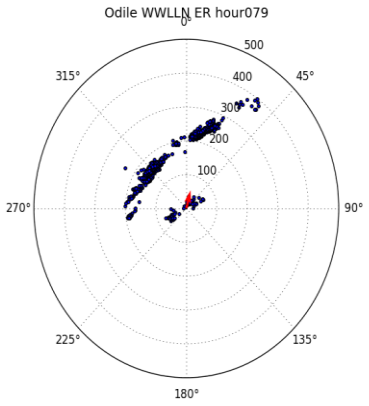

Figure 7: An hour of lightning in Hurricane Odile where eyewall lightning was occurring in opposite quadrants. This occurred during the beginning stage of an eyewall replacement cycle.

associated with mesovoticies documented in observations (Eastin et al. 2005) and modeled (Braun et al. 2006; Cram et al. 2007) may be the source of these lightning burst. This suggests lightning bursts may be indicating eye-to-eyewall horizontal mixing. In none of the storms examined, did a single burst at any time maintain itself long enough to produce lightning and completely rotate around the storm. In most cases, the lightning would be seen in one convective tower, with the lightning persisting in that area for 2-3 hours before seemingly dissipating. Hurricane Odile had one period where the lightning in the eyewall exhibited a wave number two pattern, which coincided with the beginning stages an eyewall replacement cycle (ERC) – another example of eyewall mixing. Hurricane Odile's ERC was not completed before it made landfall on the Baja California Peninsula and so the effects of land cannot be neglected. Near the onset of the ERC, lightning bursts were present in both the storm relative front-right and rear-left quadrants of the storm which can be seen in Figure 7. It is important to note that since WWLLN detects primarily CGs, IC lightning could be continuously pulsing in the eyewall and going undetected.

An examination of the lightning relative to shear vectors coincides with the results of previous research. A maxima in lightning within the eyewall tended to occur downshear for each storm with the downshear left quadrant receiving the most flashes (Corbosiero and Molinari 2002). For most of the time periods examined, shear was low and the maximum of eyewall lightning shifted slightly upshear left. Updrafts intensify in the downshear right quadrant and rotate around the eyewall reaching a peak in strength downshear left (DeHart et al. 2014). Figure 9 shows the lightning over the duration of both Raymond and Odile relative to hourly shear vectors. A large amount of Raymond's lightning occurred between 24 Oct 0000 UTC through 26 Oct 1200 UTC when Raymond was undergoing redevelopment which caused the downshear right maxima. The secondary maxima in lightning for Raymond in the downshear left quadrant occurred during its intensification periods. For low sheared storms such as Hurricane Odile, eyewall lightning actually occurred slightly in the upshear left quadrant. Lightning within the

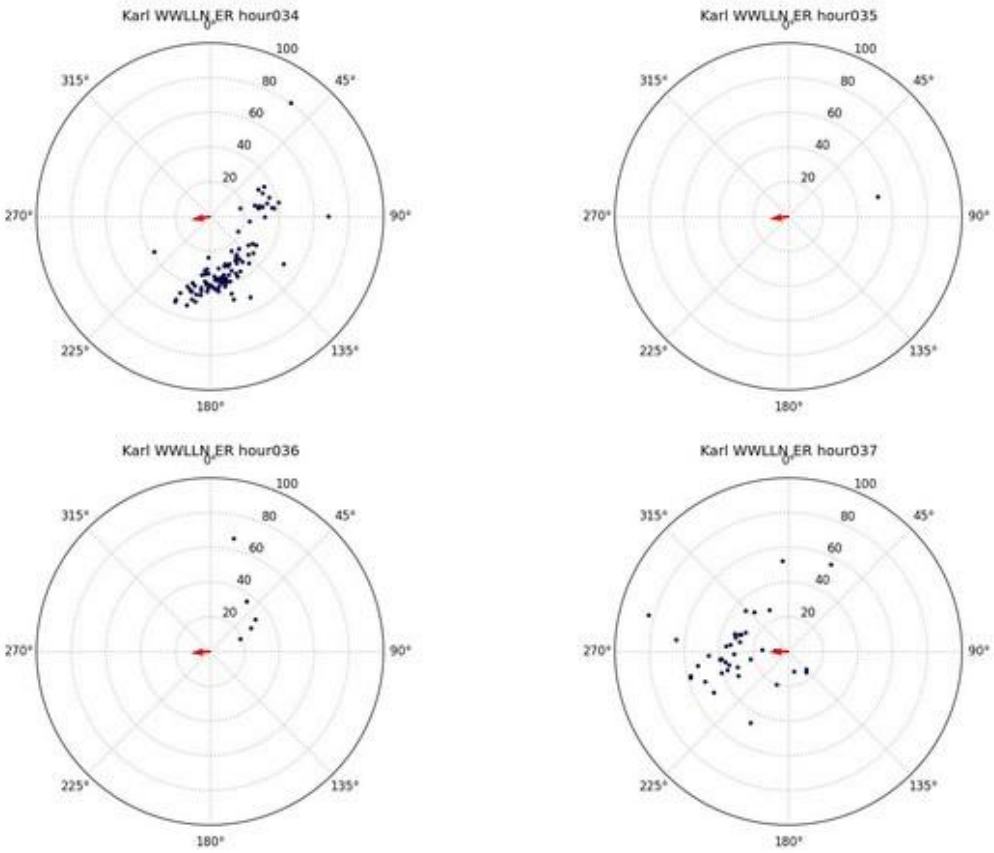

Figure 8: Hourly progressions of lightning within 100 km of Hurricane Karl's center in relation to its storm motion. Bursts of lightning never persisted long enough to track around the storm center.

rainbands did not show the same relationship and was highly variable between TC cases. Because the shear vector used was located at the center of the storm, the local shear vector in the rainband convection could not be determined, leaving further rainband lightning vs vertical wind shear relationships unresolved.

It is well documented that low shear is a necessary requirement for intensification of a tropical disturbance, but it is also plays a part in enhancing charge layers. By examining the shear vectors of each TC, we found that when a decrease in shear occurred, subsequent bursts of lightning in the eyewall corresponded to intensification. This can be seen easily in Figure 4 where the shear exceeded 15 kts during the beginning time periods for Hurricanes Odile and Blanca as the storms remained in a relatively steady state. Stronger shear persisted over several time periods in the hurricanes examined and eyewall lightning still occurred. This eyewall lightning could have been more of a product of higher shear than of convective updrafts and so

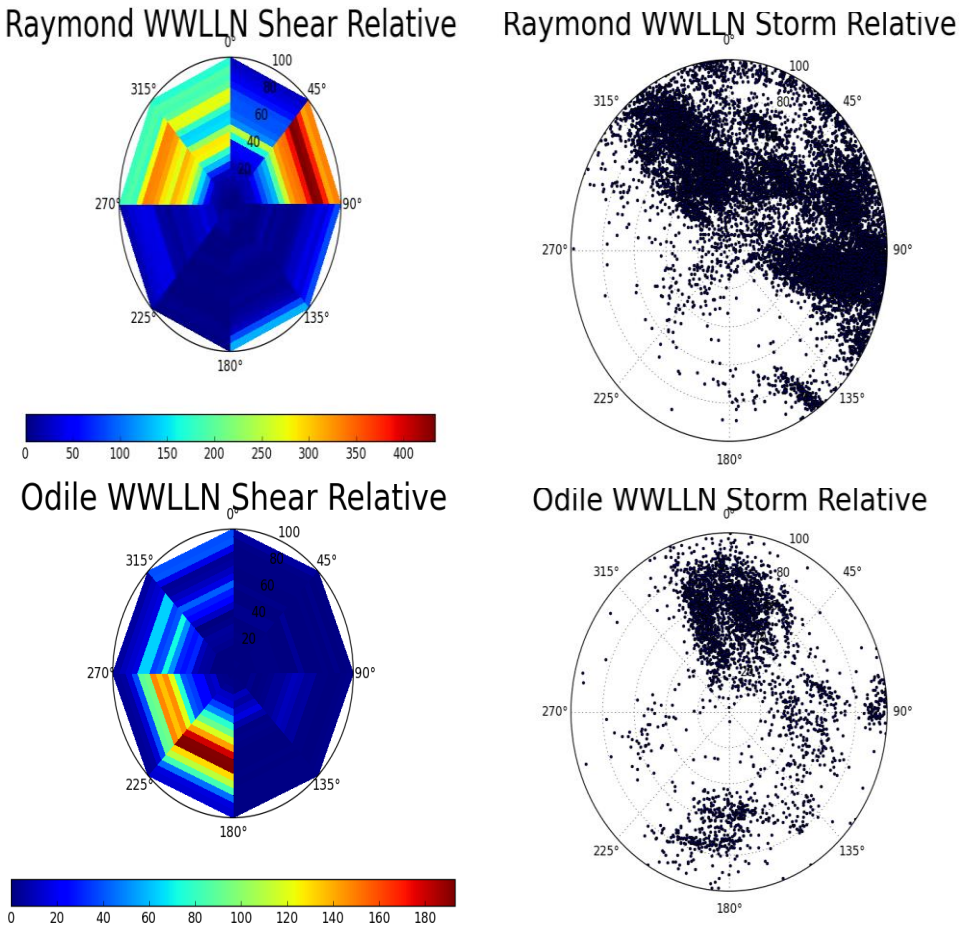

Figure 9: The left panels are WWLLN lightning over the entire examined time frame of Hurricane Odile (2014) and Hurricane Raymond (2013) relative to storm motion. Lightning is shown radially out from the storm center to 100 km. The right panels are WWLLN lightning over the entire examined time frame of the eyewall and inner core relative to a northward pointing wind shear vector.

the lightning was not indicative of intensification. When there is low shear, lightning is indicative of updraft strengths, in contrast to lightning being enhanced by strong shear. This implies that accurate shear estimates may need to be examined along with the lightning data to get the correct signal. As a result, lightning data alone, especially since the ground based detection networks detect mostly CGs, may not signal intensification, if there are high amounts of shear.

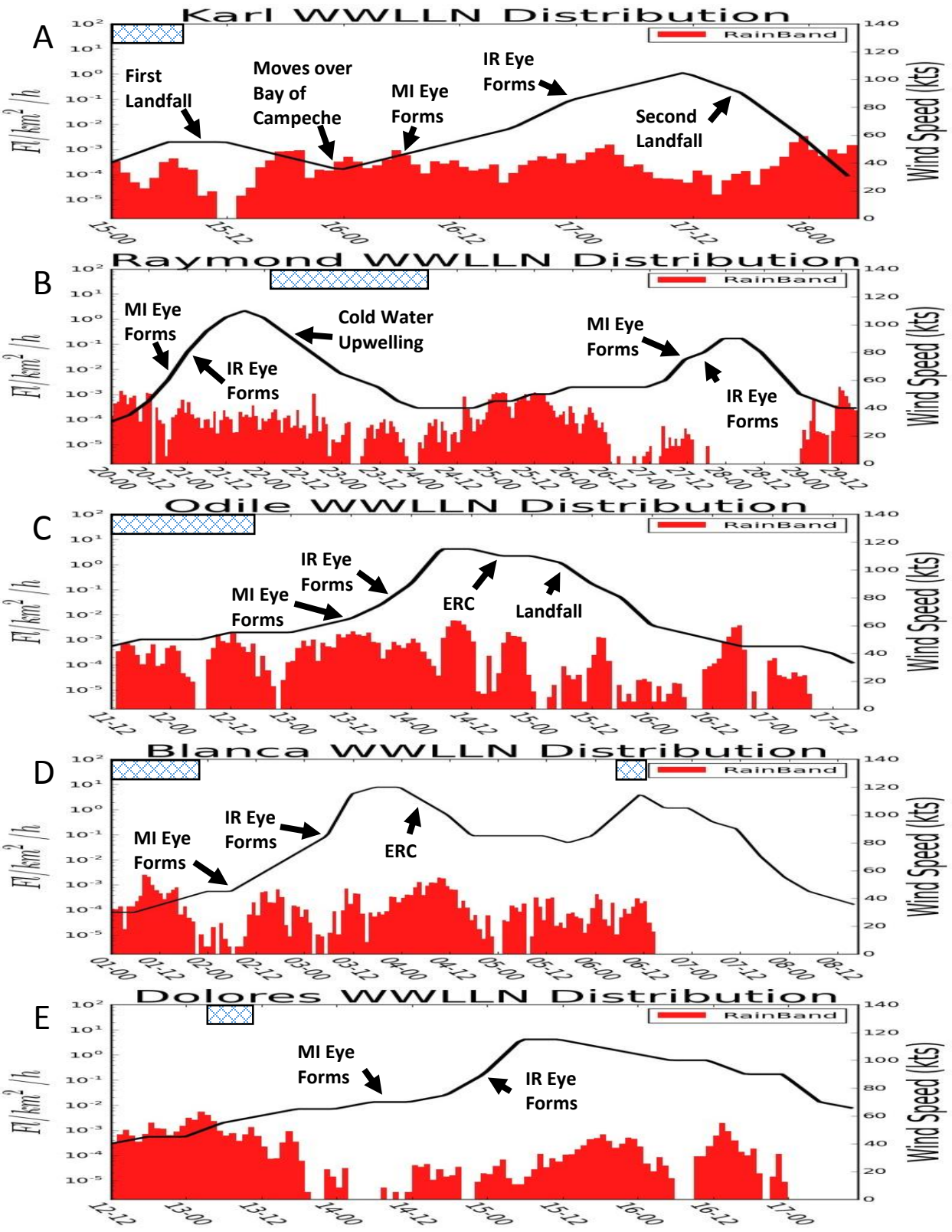

Figure 10: Temporal lightning distribution showing rainband (red) lightning in Hurricanes Karl (A), Raymond (B), Odile (C), Blanca (D), and Dolores (E) in relation to wind speed. The blue hatched area at the top of each graph shows the time period where shear is >15 kts.

b. *Rainband Lightning*

Rainband lightning patterns were very hard to discern because they were highly variable in each individual storm. Azimuthal averages of the rainband lightning show a very sporadic trend that seems to follow an almost diurnal pattern. For Hurricanes Karl, Blanca, and Delores, there may be a weak inverse relationship between rainband lightning trends and intensity trends near the peak in intensity. Just prior to peak intensity of these storms, rainband lightning starts a general decreasing trend; however, the lightning begins an increasing trend in the rainbands as the storm starts to weaken. This relationship was only seen at peak intensity and only near the end of three out of the seven RI periods. This potential signal is not consistent and could be simply contributed to general variability. A weak trend in rainband lightning, such as the cases in Karl, Blanca, and Delores, is not a useful indicators of intensity change because it cannot be easily distinguished from the many other increases and decreases in rainband lightning activity shown in Figure 10.

The examination of the rainbands is complicated in this study due to the interactions of land during some time periods. A majority of the examined time of Hurricane Karl had land interactions which can be seen in Figure 1. However, the closeness of land was a requirement for storm selection due to the intersecting domains of WWLLN and ENTLN. The importance of rainband lightning will be further evaluated in future work.

4. **Conclusion**

Although the processes that produce lightning probably have little effect on the energetics affecting strengthening or weakening of TCs, it does indicate the occurrence of deep convection and enhanced updrafts in low shear environments, which may signal the result of forces that do affect changes in TC intensity. As an indicator for intense eyewall convection and upward motion, lightning could be an important factor that could aid in the prediction of TC intensity changes. The launch of GOES-R equipped with the GLM and the increasing detection efficiency of ground-based lightning detection networks will allow for these results to be reexamined and possibly improved upon in the near future.

The current ground-based lightning detection networks are both viable options for evaluating lightning activity within tropical cyclones; however there is room for improvement. Both WWLLN and ENTLN datasets showed similar patterns in total lightning that validates the

independent use of either network for analysis. In the terms of using flash density with reliable location accuracies, both networks are suitable. The flash classification by ENTLN may need to be improved upon and stated that this information may only be valid over land. Future work needs to be done to further evaluate the accuracy of lightning data over the open ocean.

For the cases examined, results show that RI follows a burst of lightning in the eyewall when coinciding with a period of little environmental vertical shear. Eyewall/inner-core lightning is associated with deep convection and strong updrafts in low shear environments (< 15 kts) that promote intensification of TCs. This would help to explain the reason why weaker systems have higher flash densities (Abarca et al. 2010). Bursts of lightning were found to pulse prior to, during, and at the conclusion of RI. The time between pulses tended to decrease as RI was occurring and the time between eyewall pulses after RI tended to be much longer or nonexistent. Findings also show that a burst in lightning observed in the eyewall could be used to signal eye formation in both the infrared and microwave imagery and often indicate structural changes in the inner-core. Eyewall lightning tends to form in the front-right quadrant with respect to motion and then rotate to the storm's rear, mimicking observations and modeled mesovorticies, which may mix eye and eyewall air masses and promote further intensification.

The burst of eyewall lightning preceding and following a RI could be due to a change in the height of charged particles. Fierro et al. (2010) found that narrow bipolar events (NBEs), which are a type of IC discharge, showed a correlation between increases in discharge height during the deepening of Hurricane Rita and a decrease in discharge height at the conclusion of RI. An elevation of charged particles in the eyewall of a hurricane would cause more ICs and less CGs. Because both networks cannot adequately detect ICs especially over the ocean, lightning activity may be active during the entire intensification period within the eyewall. We would expect bursts of CGs occurring when charge layers are closest to the surface and ICs occurring when it is elevated. To explain the pulsing in eyewall lightning that occurs during RI, we use the evolution of updrafts.

Lightning seems to be correlated to updraft strength. The bursts of lightning that occurs during RI in the eyewall of TCs are likely occurring while these updrafts are at maximum intensity. The pulsing of lightning within the RI time period would be due to the development, intensification, and weakening of updrafts. The maximum in lightning that is seen in the downshear left quadrant is where the strongest updrafts are located. Due to similar time scales,

we propose that eyewall lightning pulses are indicators of updrafts reaching maturity. The reason that lightning within the eyewall ends following RI could be due to the disruption of updraft intensification. Therefore, the location of lightning within the eyewall may have a greater importance in distinguishing intensifying vs non-intensifying cases. Further examination of the location of bursts of lightning relative to the storm center and shear will need to be conducted with better temporal and spatial resolution.

The goal of this study is to expand on the potential use of lightning in the prediction of TC intensity changes. This has implications for incorporating a lightning predictor for forecast models in preparation for GLM.

Acknowledgements

The internship where this work was conducted was funded by NOAA. Thanks to S. Prinzivalli and W. Callahan from Earth Networks Inc. for the ENTLN data. Thanks to R. Holzworth for the WWLLN data. The views, opinions, and findings contained in this report are those of the authors and should not be construed as an official National Oceanic and Atmospheric Administration or U.S. Government position, policy, or decision.

References

Abarca, S. F., K. L. Corbosiero, and D. Vollaro, 2011: The World Wide Lightning Location Network and convective activity in tropical cyclones. *Mon. Wea. Rev*., **139**, 175-191.

Black, R.A., and J. Hallet, 1999: Electrification in hurricanes. *J. Atmos. Sci*., **56**, 2004-2028.

Braun, S. A., M. T. Montgomery, and Z. Pu, 2006: High-resolution simulation of Hurricane Bonnie (1998). Part I: The organization of eyewall vertical motion. *J. Atmos. Sci.*, **63,** 19–42.

Cram, T. A., J. Persing, M. T. Montgomery, and S. A. Braun, 2007: A Lagrangian trajectory view on transport and mixing processes between the eye, eyewall, and environment using a high resolution simulation of Hurricane Bonnie (1998). *J. Atmos. Sci*., **64**, 1835–1856.

Cangialosi, J. P. and J. L. Franklin, 2014 National Hurricane Center Forecast Verification Report. 82pp. [Available on-line at http://www.nhc.noaa.gov/verification/pdfs/Verification_2014.pdf]

Corbosiero, K. L., and J. Molinari, 2002: The effects of vertical wind shear on the distribution of convection in tropical cyclones. *Mon. Wea. Rev.*, **130**, 2110-2123.

DeHart, J. C., R. A. Houze Jr., and R. F. Rogers, 2014: Quadrant distribution of tropical cyclone inner-core kinematics in relation to environmental shear. J. Atmos. Sci., 71, 2713–2732, doi:10.1175/JAS-D-13-0298.1.

DeMaria, M., M. Mainelli, L.K. Shay, J.A. Knaff, J. Kaplan, 2005: Further Improvement to the Statistical Hurricane Intensity Prediction Scheme (SHIPS).*Wea. Forecasting*, **20**, 531-543.

DeMaria, M., R.T. DeMaria, J.A. Knaff and D.A. Molenar, 2012: Tropical cyclone lightning and rapid intensity change. *Mon. Wea. Rev*., **140**, 1828-1842.

DeMaria, M., C.R. Sampson, J.A. Knaff and K.D. Musgrave, 2014: Is tropical cyclone intensity guidance improving? *Bull. Amer. Meteor. Soc*., **95**, 387-398. Doi: http://dx.doi.org/10.1175/BAMS-D-12-00240.1

Dowden, R. L., J. B. Brundell, and C. J. Rodger, 2002: VLF lightning location by time of group arrival (TOGA) at multiple sites. *J. Atmos. Sol. Terr. Phys*., **64**, 817–830.

Eastin M. D., W. M. Gray, and P. G. Black, 2005: Buoyancy of convective vertical motions in the inner core intense hurricanes. Part II: Case Studies. *Monthly Weather Review*, **133**, 188-208.

Fierro, A. O., X-M. Shao, J. M. Reisner, J. D. Harlin and T. Hamlin, 2011: Evolution of eyewall convective events as indicated by intra-cloud and cloud-to-ground lightning activity during the rapid intensification of Hurricanes Rita and Katrina. *Mon. Wea. Rev*., **139**, 1492-1504.

Kaplan, J., M. DeMaria and J. A. Knaff, 2010: A Revised Tropical Cyclone Rapid Intensification Index for the Atlantic and Eastern North Pacific Basins. *Wea. Forcasting*, **25**, 220-241

Goodman, S. J., R. J. Blakeslee, W. J. Koshak, D. Mach, J. Bailey, D. Buechler, L. Carey, C. Schultz, M. Bateman, E. McCaul Jr., and G. Stano, 2013: The GOES-R Geostationary Lightning Mapper (GLM). *Atmos. Research*, **125-126,** 34-49. Doi:10.1016/j.atmosres.2013.01.006

Mallicka, S., V.A. Rakova,∗, J.D. Hilla,b, T. Ngina, W.R. Gamerotaa, J.T. Pilkeya,D.M. Jordana, M.A. Umana, S. Heckmanc, C.D. Sloopc, and C. Liu, 2014: Performance characteristics of the ENTLN evaluated using rocket-triggered lightning data. *Electric Power Systems Research*, **118**, 15–28

Molinari, J., P.K. Moore, V.P. Idone, R.W. Henderson, and A.B. Saljoughy, 1994: Cloud-to-ground lightning in hurricane Andrew. *J. of Geophys. Res.*, **99**, 16665-16676.

Rodger, C. J., S. Werner, J. B. Brundell, E. H. Lay, N. R. Thompson, R. H. Holzworth, and R. L. Dowden, 2006: Detection efficiency of the VLF World-Wide Lightning Location Network (WWLLN): Initial case study. *Ann. Geophys.*, **24**, 3197–3214.

Rodger, C.J.; Brundell, J.B.; Hutchins, M.; Holzworth, R.H., 2014: The world wide lightning location network (WWLLN): Update of status and applications. *General Assembly and Scientific Symposium (URSI GASS), 2014 XXXIth URSI* , 16-23 Aug. 2014, 1-2, doi: 10.1109/URSIGASS.2014.6929581

Rogers, R., S. Lorsolo, P. Reasor, J. Gamache, and F. Marks, 2012: Multiscale analysis of tropical cyclone kinematic structure from airborne Doppler radar composites. *Mon. Wea. Rev.*, **140**, 77–99. Doi: http://dx.doi.org/10.1175/MWR-D-10-05075.1

Rogers, R., P. Reasor, and S, Lorsolo, 2013: Airborne Doppler observations of the inner-core structural differences between intensifying and steady-state tropical cyclones. *Mon. Wea. Rev.*, **141**, 2970–2991. Doi: http://dx.doi.org/10.1175/MWR-D-12-00357.1

Rudlosky, S. D., and D. T. Shea, 2013: Evaluating WWLLN Performance Relative to TRMM/LIS,*Geophys. Res. Lett*., **40**, 2344–2348, doi:10.1002/grl.50428.

Rudlosky, S. D., 2014: Evaluating ground-based lightning detection networks using TRMM/LIS observations, 23rd International Lightning Detection Conference & 5th International Lightning Meteorology Conference, Vaisala Inc., Tucson, Ariz.

SHIPS, 2015: SHIPS Developmental Data. [Available on-line at http://rammb.cira.colostate.edu/research/tropical_cyclones/ships/developmental_data.asp]

Solorzano, N. N., H. N. Thomas, and R. H. Holzworth, 2008: Global studies of tropical cyclones using the World Wide Lightning Location Network. [Available online at http://wwlln.net/publications/Solorzano_AMS_29FEB2008.pdf]

Squires, K., and S. Businger, 2008: The morphology of eyewall lightning outbreaks in two category 5 hurricanes. *Mon. Wea. Rev*., **136**, 1706-1726.

Uhlhorn, E.W., B.W. Klotz, T. Vukicevic, P.D. Reasor, and R.F. Rogers, 2014: Observed hurricane wind speed asymmetries and relationships to motion and environmental shear. *Mon. Wea. Rev*., **142**, 1290-1311. Doi:10.1175/MWR-D-13-00249.1